ENGINEERING TRANSACTIONS • *Engng. Trans.* • **63**, 1, 55–76, 2015
Polish Academy of Sciences • Institute of Fundamental Technological Research (IPPT PAN)
National Engineering School of Metz (ENIM) • Poznan University of Technology

Two-Scale Modelling of Reactive Powder Concrete. Part III: Experimental Tests and Validation

Arkadiusz DENISIEWICZ[1)], Mieczysław KUCZMA[2)]

[1)] *University of Zielona Góra*
Division of Structural Mechanics
Prof. Z. Szafrana 1, 65-246 Zielona Góra, Poland
e-mail: a.denisiewicz@ib.uz.zgora.pl

[2)] *Poznan University of Technology*
Institute of Structural Engineering
Piotrowo 5, 61-965 Poznań, Poland
e-mail: mieczyslaw.kuczma@put.poznan.pl

This article is the third and final part of a series about two-scale modelling of reactive powder concrete in the linear range. In the first part [1] a method of modelling RPC microstructure was presented, the boundary value problem of mechanics for a representative cell at the micro scale was formulated and solved. In the second part [2] a method for determining material parameters at the macro level was shown, a technique for enforcing boundary conditions upon an RVE was described, and the results of numerical simulations were presented. In this part we will present the results of laboratory tests of full-size beams made from two RPC mixtures, the results of numerical simulations of these beams and the validation of the proposed numerical model.

Key words: two-scale modelling, numerical homogenization, RPC, FEM, numerical simulations, experimental tests.

1. Recipes of RPC

For the purpose of validation of the RPC numerical model, two mixtures were prepared with different components and a number of samples were made and subjected to laboratory tests. The results were used to validate the proposed theoretical model.

The course of action while preparing reactive powder concrete is completely different from that for traditional concrete. The reason is that the known equations (by Bolomey, Abrams, etc.) used to determine strength depending on the components became invalid because of the low values of the W/B ratio for RPC. Consistency equations are no longer true either because of the large amount of superplasticizers in the mixture. The only relationship that is still true is the

so-called water tightness equation [14]. In the author's opinion [14] the best method used to determine RPC recipes is by experiment.

In this paper the recipes were initially determined on the basis of literature as well as the water tightness equation adequately extended for a particular mixture,

$$\frac{C}{\rho_C}+\frac{Pk}{\rho_{Pk}}+\frac{P_I}{\rho_{P_I}}+\frac{P_{II}}{\rho_{P_{II}}}+\frac{P_{III}}{\rho_{P_{III}}}+\frac{F}{\rho_F}+\frac{MF}{\rho_{MF}}+\frac{S}{\rho_S}+\frac{W}{\rho_W}=1, \tag{1.1}$$

where C, Pk, P_I, P_{II}, P_{III}, F, MF, S, W – amounts [kg/m^3] of: cement, silica powder, OS – 30 sand, OS – 36 sand, OS – 38 sand, steel fibres, steel micro fibres, superplasticizer, water ρ_C, ρ_{Pk}, ρ_{P_I}, $\rho_{P_{II}}$, $\rho_{P_{III}}$, ρ_F, ρ_{MF}, ρ_S, ρ_W – density [kg/m^3] of: cement, silica powder, OS – 30 sand, OS – 36 sand, OS – 38 sand, steel fibres, steel micro fibres, superplasticizer, water.

While preparing the recipes, we made also use of the formulae applied to determine the strength of high strength concrete. One of them was the de Larrard equation [7, 6],

$$f_{c28}=\frac{k_k k_c}{\left[\dfrac{1+3.1\,W/C}{1.4-0.4\exp(-11\,Pk/C)}\right]^2}, \tag{1.2}$$

where k_k – the coefficient dependent on the type of aggregate, k_c – the strength of cement [MPa], and the other designations as in (1.1). Another equation taken into account is the modified de Larrard relationship, which is adapted to the specificity of Polish aggregates [8]

$$f_{c28}=\frac{k_k k_c}{\left[1+3.1\dfrac{0.4\,W/C}{1.4-0.4\exp(-11\cdot 2.25\,Pk/C)}\right]^2}. \tag{1.3}$$

In order to estimate the compressive strength of the completed RPC, an equation from the publication [15] was used

$$f_{c28}=\frac{188.4}{21.7^{\left(\frac{W}{C+Pk}-0.15\frac{Pk}{C}\right)}}. \tag{1.4}$$

Because of restrictions on the use of the above-mentioned equations they were used as an auxiliary way to estimate the amount of cement and silica powder necessary to achieve the expected strengths.

Before proper samples were made, test batches of concrete had been prepared in order to check the recipes. During those tests it was found that it was necessary to increase the admixture of superplasticizer from 1% (9 litres/m^3) to 3.3% (29.6 litres/m^3) of the cement mass. The initial amount of superplasticizer had been recommended by the manufacturer. However, in the case of RPC the amount was insufficient to provide good workability of the mixture because

this type of concrete has a low water/binding ratio. Two test batches of concrete were prepared based on the recipe "mixture I" (Table 2). Altogether five samples with dimensions 15×15×15 cm were prepared, consistent with the standards [8, 9]. The first batch was prepared without a fibre admixture and with an initially adopted amount of fluidifying admixture. Figure 1 clearly shows concentrations of non-hydrated cement granules, which are a result of an insufficient amount of fluidifying admixture. This caused an insufficient distribution of components in spite of a long mixing time (25 min). The second test batch contained both kinds of fibres and the target amount of superplasticizer. During mixing the required amount of this admixture was controlled until good workability was achieved. Seven days after forming, compressive strength tests were conducted. The results are presented in Table 1.

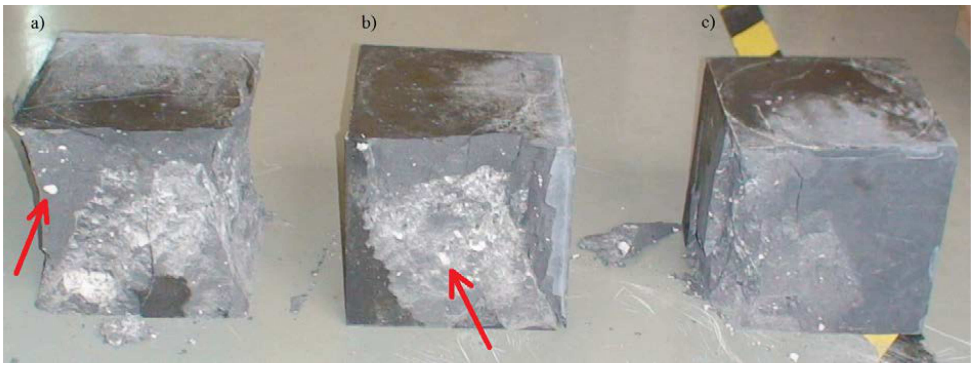

FIG. 1. Destroyed samples from the test batch without fibres:
a) sample No. 1, b) sample No. 2, c) sample No. 3.

Table 1. The results of compressive strength tests conducted on samples from the first test batch.

Sample No.	Steel fibre and micro fibre admixture	Compressive strength after 7 days [MPa]	Average strength [MPa]
1	NO	81.87	80.54
2	NO	84.97	
3	NO	74.77	
4	YES	102.5	100.88
5	YES	99.25	

As expected, the strength of RPC with steel fibres was considerably higher ($\approx 20\%$) than the strength of samples without this admixture. Samples 1–3 can be characterised as undergoing damage typical of brittle materials i.e. after reaching their load capacity they were no longer able to bear load (they were destroyed). Samples 4 and 5 behaved differently, exhibiting some features of plasticity.

During the strength test the effects of material flow and plastic strengthening were clearly seen. The samples were not destroyed after reaching their compressive strength capacity. The loss of compressive strength capacity resulted in minor cracks (Fig. 2), which did not lead to the loss of material stability.

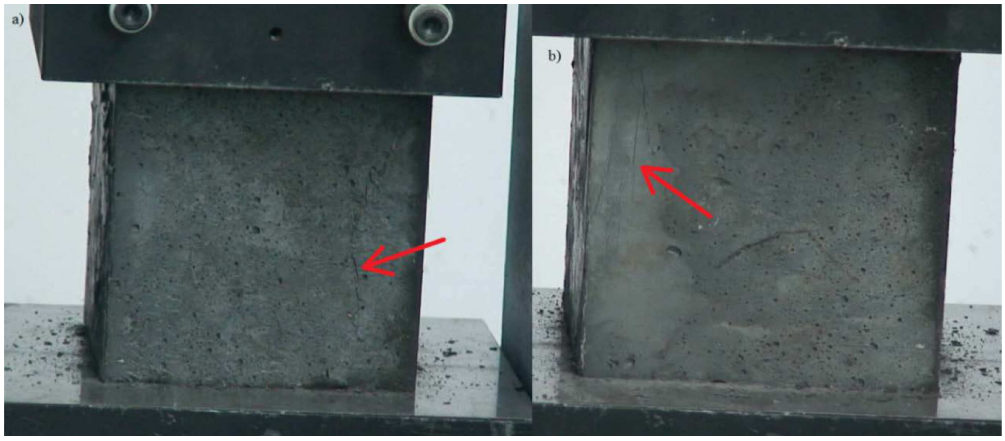

FIG. 2. Destroyed samples from the test batch with fibres: a) sample No. 4, b) sample No. 5.

After the analysis of the test batches, the recipes for target components shown in Table 2 were adopted, with the basic mixture parameters given in Table 3 and the estimated compressive strength in Table 4.

Table 2. Recipes.

Component	Mixture I [kg/m^3]	Percent amount [%]	Mixture II [kg/m^3]	Percent amount [%]
Cement CEM I 42,5R	905	34.2	905	33.2
Silica fume	230	8.7	230	8.4
Quartz sand 0.063–0.4 mm OS 36	702	26.6	330	12.1
Quartz sand 0.04–0.125 mm OS 38	285	10.8	285	10.5
Quartz sand 0.2–0.8 mm OS 30	–	–	335	12.3
Water	260	9.8	260	9.5
Superplasticizer Woerment FM 787 BASF®	29.6	1.1	29.6	1.1
Micro steel fibres DM 6/0.17 KrampeHarex®	233	8.8	233	8.6
Steel fibres DW 38/1.0 N KrampeHarex®	–	–	117	4.3
Densities	2645	–	2725	–

Table 3. Basic mixture parameters.

Parameter	Mixture I	Mixture II
W/B	0.29	0.29
W/B	0.23	0.23
Pk/C	0.25	0.25
Amount of superplasticizer per cement mass	3.3%	3.3%
Amount of superplasticizer per binding material mass	2.6%	2.6%

Table 4. Theoretical compressive strength after 28 days.

Basis for estimation	Estimated compressive strength f_{c28} [MPa]	
	Mixture I	Mixture II
Equation (1.2)	125.24	125.24
Equation (1.3)	100.44	100.44
Equation (1.4)	104.68	104.68

2. Kinds of samples and the research programme

Altogether 32 samples were prepared for strength tests and they consist of 3 kinds: a beam, a small-sized beam and a cube (Table 5), and were made from two kinds of mixtures (Table 2).

Table 5. Selection of samples prepared for laboratory tests.

Type of sample	Dimensions of sample [cm]	Quantity of samples	
		Mixture I	Mixture II
Beam	10×15×200	4	4
Small-sized beam	10×10×46	6	6
Cube	10×10×10	6	6
	Altogether	32	

The following sample designations were adopted:

- B1-M1 ÷ B4-M1 – beams of dimensions 10×15×200 cm, made from mixture I,
- B1-M2 ÷ B4-M2 – beams of dimensions 10×15×200 cm, made from mixture II,
- P1-M1 ÷ P6-M1 – small-sized beams of dimensions 10×10×46 cm, made from mixture I,

- P1-M2 ÷ P6-M2 – small-sized beams of dimensions 10×10×46 cm, made from mixture II,
- K1-M1 ÷ K6-M1 – cubes of dimensions 10×10×10 cm, made from mixture I,
- K1-M2 ÷ K6-M2 – cubes of dimensions 10×10×10 cm, made from mixture II.

The research programme was divided into six stages:

1) preparation of test batches to verify the proposed recipes,
2) compressive strength tests (after 7 days) conducted on samples from the test batch by means of a hydraulic press with the capacity of 3000 kN,
3) preparation of target samples,

Table 6. Types of response to enforced middle-span displacements [mm] in beams: green – linear elastic, orange – non-linear, blue – collapse.

Beam B1-M1		Beams B2-M1, B3-M1, B4-M1		Beam B1-M2		Beams B2-M2, B3-M2, B4-M2	
Displacement	Sample	Displacement	Sample	Displacement	Sample	Displacement	Sample
0.1	B1-M1	0.25	B2-M1 B3-M1 B4-M1	0.25	B1-M2	0.50	B2-M2 B3-M2 B4-M2
0.2	B1-M1_2	0.25	B2-M1_2 B3-M1_2 B4-M1_2	0.25	B1-M2_2	0.50	B2-M2_2 B3-M2_2 B4-M2_2
0.3	B1-M1_3	0.50	B2-M1_3 B3-M1_3 B4-M1_3	0.50	B1-M2_3	0.75	B2-M2_3 B3-M2_3 B4-M2_3
0.4	B1-M1_4	0.75	B2-M1_4 B3-M1_4 B4-M1_4	0.75	B1-M2_4	1.00	B2-M2_4 B3-M2_4 B4-M2_4
0.5	B1-M1_5	1.00	B2-M1_5 B3-M1_5 B4-M1_5	1.00	B1-M2_5	1.25	B2-M2_5 B3-M2_5 B4-M2_5
0.6	B1-M1_6	1.25	B2-M1_6 B3-M1_6 B4-M1_6	1.25	B1-M2_6	1.50	B2-M2_6 B3-M2_6 B4-M2_6
0.7	B1-M1_7	1.50	B2-M1_7 B3-M1_7 B4-M1_7	1.50	B1-M2_7	1.75	B2-M2_7 B3-M2_7 B4-M2_7
0.8	B1-M1_8	1.75	B2-M1_8 B3-M1_8 B4-M1_8	1.75	B1-M2_8	2.00	B2-M2_8 B3-M2_8 B4-M2_8
0.9	B1-M1_9	16.0	B2-M1_9 B3-M1_9 B4-M1_9	2.00	B1-M2_9	16.0	B2-M2_9 B3-M2_9 B4-M2_9
1.0	B1-M1_10	–	–	16.0	B1-M2_10	–	–
1.2	B1-M1_11	–	–	–	–	–	–
1.4	B1-M1_12	–	–	–	–	–	–
1.6	B1-M1_13	–	–	–	–	–	–
1.8	B1-M1_14	–	–	–	–	–	–
2.0	B1-M1_15	–	–	–	–	–	–
2.2	B1-M1_16	–	–	–	–	–	–
32.0	B1-M1_17	–	–	–	–	–	–

4) three-point bending tests until the destruction of beams B1-M1 ÷ B4-M1 and B1-M2 ÷ B4-M2 in the testing machine Instron 8804 with the capacity of ±500 kN, the deformation measurement in the destruction zone with the system Aramis 3D and checking of point deformation with electrical resistance strain gauges,
5) three-point bending tests of small-sized beams P1-M1 ÷ P6-M1 and P1-M2 ÷ P6-M2 in the testing machine Instron 8804 with the capacity of ±500 kN,
6) compressive strength tests of cubes K1-M1 ÷ K6-M1 and K1-M2 ÷ K6-M2 in a hydraulic press with the capacity of 3000 kN and simultaneous measurements of deformations in two perpendicular directions with electrical resistance strain gauges.

The bending test and the compression test were conducted in agreement with the Polish standards [10–12]. Table 6 presents the realized programme of the strength tests for samples B1-M1 ÷ B4-M1 and B1-M2 ÷ B4-M2. The linear-elastic range has been marked in green, the non-linear range in orange and the destruction test in blue.

3. Technology of sample preparation and storage

Before the test samples were prepared the components of the proposed mixtures had been carefully weighed out (with an accuracy of 10 g) The mixture preparation process was divided into four stages, with two batches from mixture I and two from mixture II. A free fall concrete mixer MK 165/B with the working capacity of 130 l was used to prepare the RPC. The whole process of mixing each batch lasted for about 25 minutes. The components were dosed according to the following procedure:

1) dry mixing for 1 minute the whole amount of silica powder with 1/3 of the amount of cement,
2) addition of 1/2 of the amount of water and the whole amount of superplasticizer (mixing until a liquid slurry was obtained),
3) addition of the remaining 2/3 of the amount of cement and the remaining amount of water (mixing until a homogeneous slurry was obtained),
4) gradual addition of steel micro fibres DM 6/0.17 (mixing until all the fibres had been "absorbed" by the mixture),
5) gradual dosage of sands in the sequence OS – 30 (only for mixture II), OS – 36 and OS – 38 (mixing until homogeneous concrete was obtained),
6) in the case of mixture II while adding sands, steel fibres were also dosed gradually DW 38/1.0 N.

After mixing the fresh concrete was immediately poured into the mould. It was made of an 18 mm thick MFP plate. Before the mixture was poured the inside of the mould had been covered with an anti-adhesive agent. While the samples were being made from mixture I the mould was subjected to vibrations (the whole mould was fastened to a vibrating table). The samples made from mixture II were condensed manually. While the concrete was curing no actions were taken. The mould with the samples was only protected against loss of moisture with a foil cover. Selected components were seasoned in this form for 28 days at the temperature of 20°C. The samples designated as K1-M1 ÷ K6-M1 and K1-M2 ÷ K6-M2 (cubes 10×10×10 cm for compressive strength tests) were placed in steel moulds and stored in a chest used for seasoning test materials.

After 28 days all the samples were taken out of the moulds and prepared for tests (Fig. 5). After preliminary preparation of cubes K1-M1 ÷ K6-M1 and K1-M2 ÷ K6-M2 (Fig. 3b, c), electrical resistance strain gauges EA-06-250BG-120 manufactured by VISHAY with the base length and width of 6.35 mm and 3.18 mm respectively were stuck to them. A two-component epoxy glue was used to fasten the strain gauges to the samples and cleaning materials from the same manufacturer. A scheme of the layout of the sensors on the sample is shown in Fig. 4a. Electrical resistance strain gauges EA-06-250BG-120 were also used during the tests of beams B1-M1 ÷ B4-M1 and B1-M2 ÷ B4-M2 (Fig. 3d). They were installed according to the scheme shown in (Fig. 4b). Moreover, at the points designated as A1, A2, A3 displacement sensors were installed in order to check the system of sample and testing machine for appearing of clearances as well as to get additional measurements of beam deflections. In the middle section of the beam (the destruction zone) a measurement area was prepared

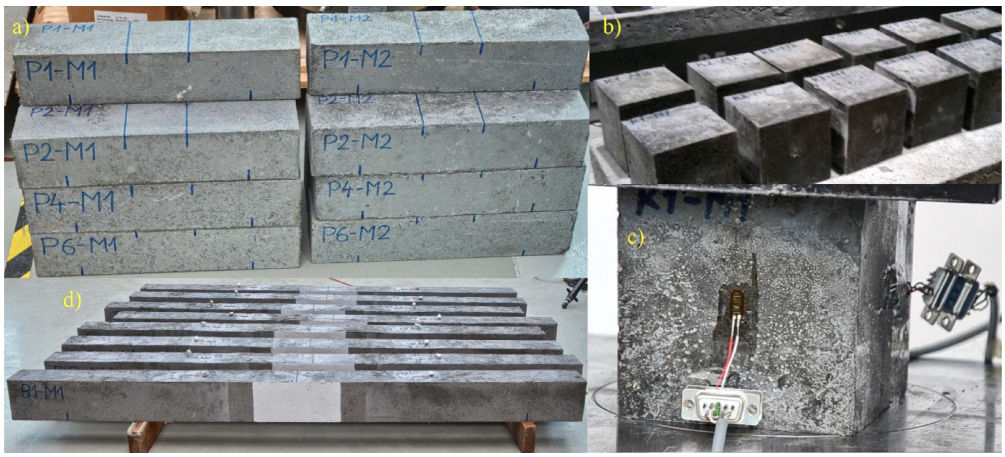

FIG. 3. Samples prepared for the tests.

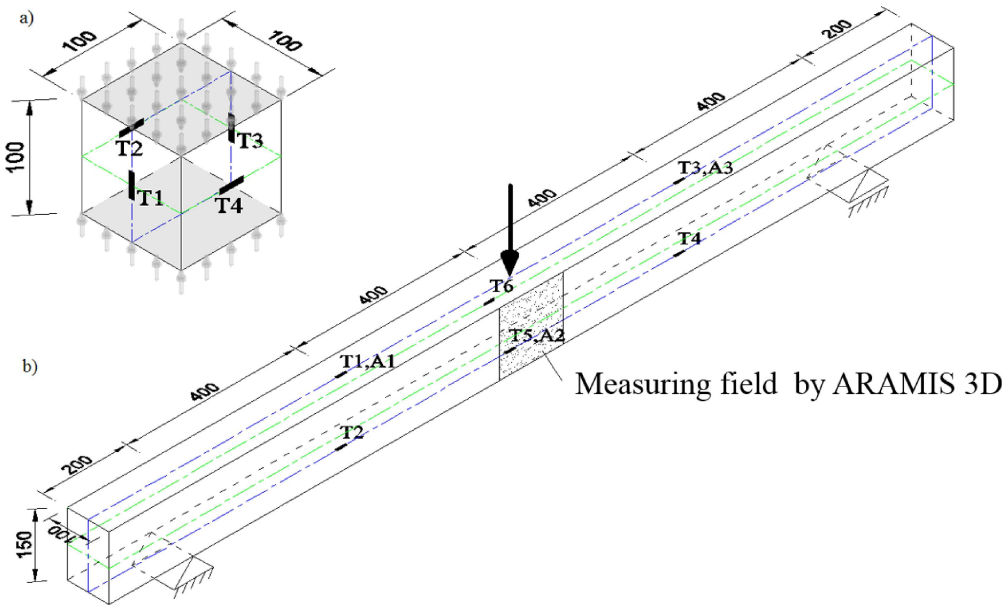

FIG. 4. A scheme of the measurements: a) cubes K1-M1 ÷ K6-M1 and K1-M2 ÷ K6-M2, b) beams B1-M1 ÷ B4-M1 and B1-M2 ÷ B4-M2, dimensions [mm].

for the optical deformation measuring system Aramis [5]. All the samples were prepared in agreement with the Polish standards [8, 9].

4. Test stands

The first test was conducted to determine the flexural strength of small-sized beams P1-M1 ÷ P6-M1 and P1-M2 ÷ P6-M2 in agreement with the Polish standard PN-EN 12390-5 [12]. The static displacement-controlled tests were conducted by using the testing machine Instron 8804 with the capacity of ±500 kN (Fig. 5). The obtained results are gathered in Table 7 and showed in Figs. 10, 11.

The second test was conducted to determine the compressive strength of cubes K1-M1 ÷ K6-M1 and K1-M2 ÷ K6-M2 in agreement with the Polish standard PN-EN 12390-3 [10]. During these tests, deformations were measured in two mutually perpendicular directions with strain gauges to determine Poisson's ratio (Fig. 6). The tests were controlled with a load increment whose velocity was 1 MPa/s ± 10%. This tolerance in controlling the velocity of load increment results from the fact that the used machine allows only for manual control of this parameter. According to the Polish standard such a deviation is acceptable. A graphical representation of the readings from the strain gauge bridge can be found in [3], and the values of Poisson's ratio and compressive strength are given in Tables 8 and 9.

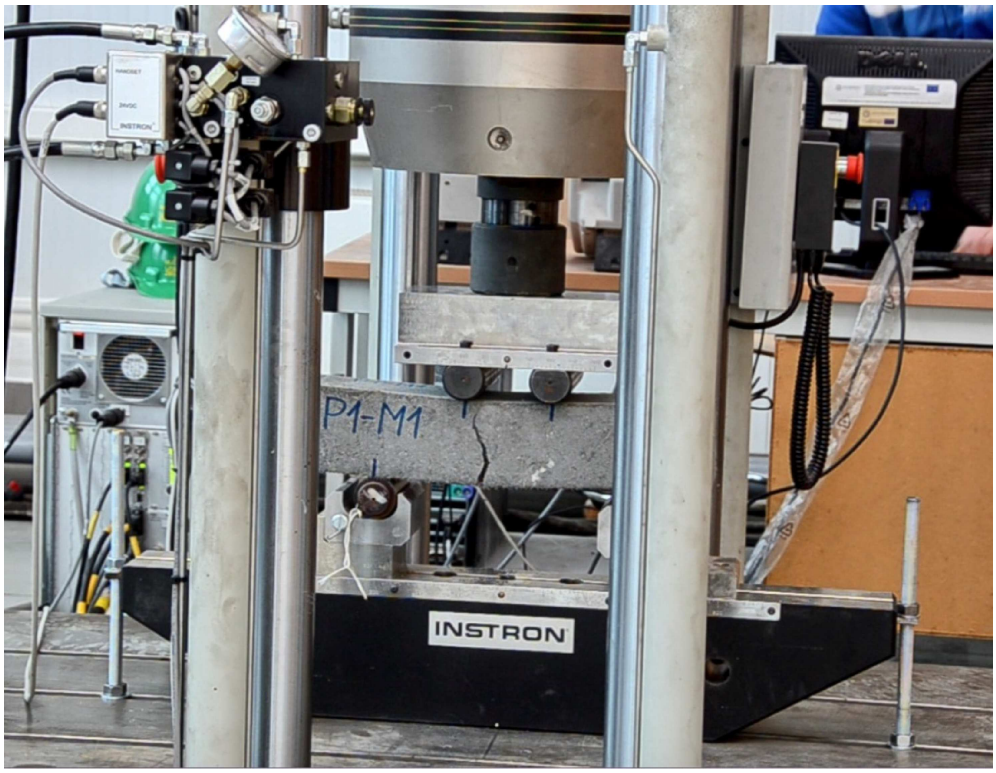

FIG. 5. The test stand for testing small-sized beams P1-M1 ÷ P6-M1 and P1-M2 ÷ P6-M2.

FIG. 6. The test stand for testing cubes K1-M1 ÷ K6-M1 and K1-M2 ÷ K6-M2.

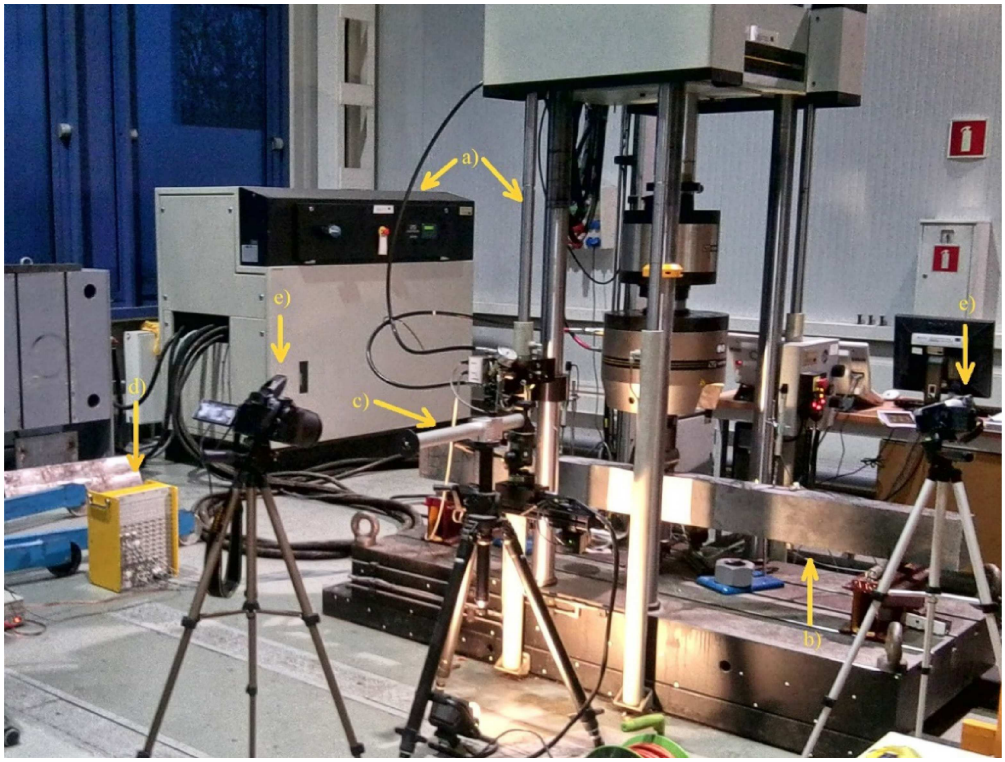

FIG. 7. The test stand for testing beams B1-M1 ÷ B4-M1 and B1-M2 ÷ B4-M2, a) testing machine Instron 8804, b) beam subjected to tests, c) cameras of the deformation measuring system Aramis 3D, d) strain gauge bridge, e) cameras recording the tests.

The third and final test was conducted to determine Young's moduli for RPC concrete made from mixture I and mixture II and to record the destruction process of the beams. It was conducted on samples B1-M1 ÷ B4-M1 and B1-M2 ÷ B4-M2. During the tests conducted with the strength test machine Instron 8804 deformations were measured with a strain gauge and the destruction zone was monitored with the system Aramis (Fig. 7). Detailed test results can be found in [3].

5. TEST RESULTS

5.1. Flexural strength tests

Table 7 presents the values of flexural strength for particular samples and averaged values. Figure 8 dipicts the diagrams of force-displacement relationships which we obtained in the tests on small-sized beams made from mixture I, whereas Fig. 9 on those made from mixture II. Figure 1 shows the destroyed

Table 7. Flexural strength.

Sample	Maximum force F [N]	Flexural strength f_{cf} [MPa]
Mixture I		
P1-M1	48770	14.63
P2-M1	50510	15.15
P3-M1	34160	10.25
P4-M1	36670	11.00
P5-M1	37560	11.27
P6-M1	42120	12.64
Mean value	**41632**	**12.49**
Mixture II		
P1-M2	57740	17.32
P2-M2	57540	17.26
P3-M2	51780	15.53
P4-M2	59410	17.82
P5-M2	65670	19.70
P6-M2	67850	20.35
Mean value	**59998**	**18.00**

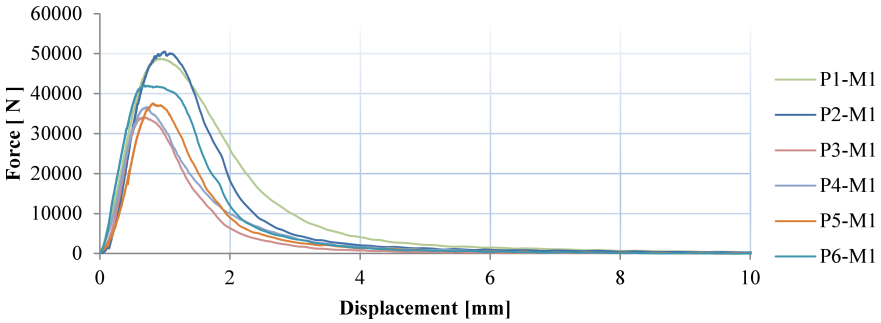

FIG. 8. Force-displacement relationships for the samples made from mixture I.

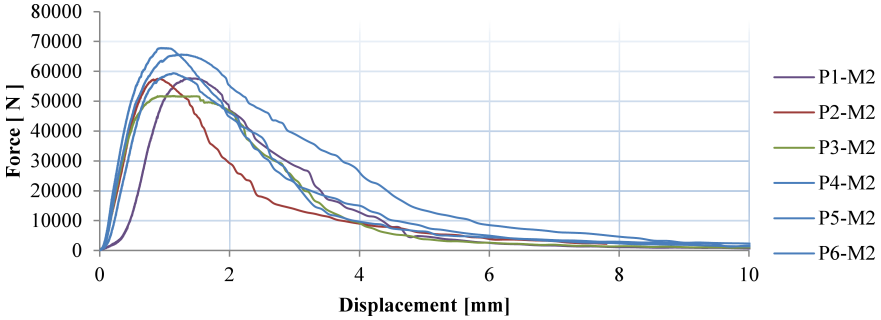

FIG. 9. Force-displacement relationships for the samples made from mixture II.

samples and close ups of the fractures. The bending strength consistent with the Polish standard [12] for a four-point bending test was determined by the formula

$$f_{cf} = \frac{F \cdot l}{d_1 \cdot d_2^2}, \tag{5.1}$$

where f_{cf} – the flexural strength [MPa], F – the maximum load [N] – load bearing capacity of the sample, l – the support spacing [mm], d_1, d_2^2 – the width and height of the sample's cross-section [mm].

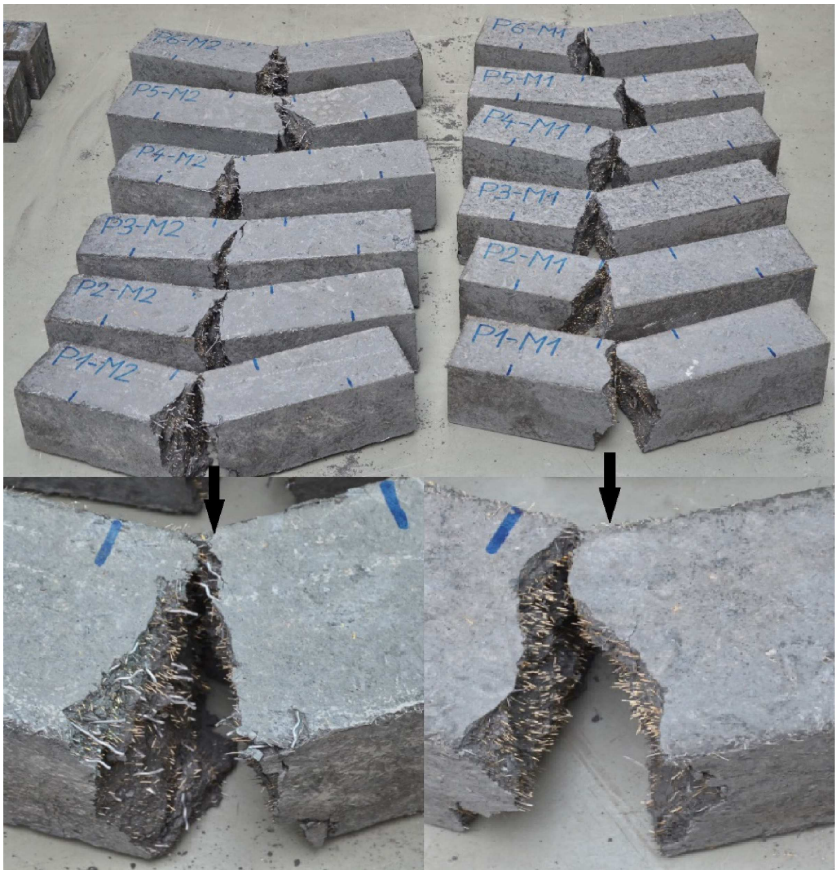

FIG. 10. Destroyed small-sized beams P1-M1 ÷ P6-M1 and P1-M2 ÷ P6-M2.

5.2. Compressive strength tests and determination of Poisson's ratio

The results of the compressive strength tests of samples K1-M1 ÷ K6-M1 and K1-M2 ÷ K6-M2 are presented in Table 8. The value of the maximum compression force and compressive strength were read from the display of the hydraulic

Table 8. Compressive strength.

Sample	Force F [kN]	Compressive strength f_c [MPa]
Mixture I		
K1-M1	1079.13	107.90
K2-M1	1044.29	104.40
K3-M1	962.88	96.29
K4-M1	1006.35	100.60
K5-M1	1134.12	113.40
K6-M1	1131.96	113.20
Mean value	**1059.79**	**105.97**
Mixture II		
K1-M2	1428.13	142.80
K2-M2	1457.94	145.80
K3-M2	1384.86	138.50
K4-M2	1373.52	137.40
K5-M2	1386.71	138.70
K6-M2	1430.76	143.10
Mean value	**1410.32**	**141.05**

press (Fig. 6). This machine calculates compressive strength in agreement with the Polish standard [10]

$$f_c = \frac{F}{A_c}, \tag{5.2}$$

where f_c – the compressive strength [MPa], F – the maximum compression force [N], A_c – the cross-sectional area of a sample [mm^2].

The values of Poisson's ratio that were determined are presented in Table 9. Figure 11 shows the destroyed cubes. Samples K2-M1, K4-M1, K2-M2, which

Table 9. Poisson's ratios for cubes made from mixture I and mixture II.

Sample	Poisson's ratio	Sample	Poisson's ratio
K1-M1	0.15	K1-M2	0.19
K2-M1	0.19	K2-M2	0.25
K3-M1	0.27	K3-M2	0.47
K4-M1	0.16	K4-M2	0.29
K5-M1	0.25	K5-M2	0.22
K6-M1	0.16	K6-M2	0.47
Mean values	**0.20**		**0.32**

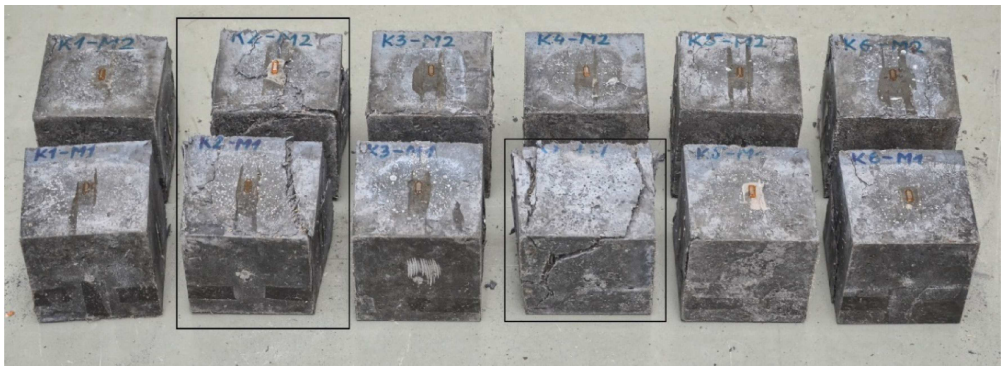

FIG. 11. Destroyed cubes K1-M1 ÷ K6-M1 and K1-M2 ÷ K6-M2, (description in the text).

are more deformed than the other samples, are marked with black rims. The observed deformations are a result of subsequent reloading, i.e. after the standard tests these samples were subjected to loading again in order to check whether they would disintegrate. Despite the clearly seen considerable fractures, no destruction typical of cubes made from traditional concrete was found. The material was still capable of bearing a compressive force (the descending branch). Despite small cracks and some chipping there is not much damage to the other samples. High elasticity of RPC is a result of the presence of a large amount of steel fibres among its ingredients (Table 2).

The result obtained for the cubes denoted as K3-M2 and K6-M2 is remarkable because it differs considerably from the other values. It is supposed that it could be a result of a specific configuration of fibres which must have occurred during the formation of the cubes. If these results were disregarded assuming that they are a result of damage or faulty operation of the strain gauges, the mean value of Poisson's ratio for mixture II would be 0.24. This value is highly probable in light of the authors' own numerical simulations and the results of research available in the literature.

5.3. Tests of beams (determining Young's modulus)

Eight beams B1-M1 ÷ B4-M1 and B1-M2 ÷ B4-M2 made from two kinds of mixture were tested. The goal of the experiment was to determine the averaged elasticity modulus of RPC and to record the destruction process of the beams during a three point bending test. The value of macro Young's modulus was determined on the basis of Hooke's law:

$$\overline{\sigma} = \overline{E}\overline{\varepsilon} \Rightarrow \overline{E} = \frac{\overline{\sigma}}{\overline{\varepsilon}}. \tag{5.3}$$

The value of deformation $\overline{\varepsilon}$ was obtained by measurements within the elastic range of loading. The stress value corresponding to a particular deformation was determined from the well-known formula,

$$\overline{\sigma} = \frac{M}{W}, \tag{5.4}$$

where M is the bending moment in the cross-section where the strain gauges were installed (0.4 m from the support see Fig. 6b). For the tested beams $M = 0.4P$ and the section modulus of the cross-section is $W = 0.000375$ m^4. Finally the formula used to calculate the elasticity modulus has the form

$$\overline{E} = \frac{533\frac{1}{3} \cdot P}{\overline{\varepsilon}}. \tag{5.5}$$

Tables 10 and 11 below present values calculated according to (5.5).

Table 10. Young's moduli [GPa] for the beams made from mixture I.

Sample	$\overline{E}$	Sample	$\overline{E}$	Sample	$\overline{E}$	Sample	$\overline{E}$
B1-M1	40.61						
B1-M1_2	41.64	B2-M1_2	38.17	B3-M1_2	41.74	B4-M1_2	45.42
B1-M1_3	39.75	B2-M1_3	38.71	B3-M1_3	42.61	B4-M1_3	42.77
B1-M1_4	42.65	B2-M1_4	41.31	B3-M1_4	42.75	B4-M1_4	45.05
B1-M1_5	41.87	B2-M1_5	42.23	B3-M1_5	45.74	B4-M1_5	44.69
B1-M1_6	41.97	–	–	–	–	–	–
B1-M1_7	43.75	–	–	–	–	–	—-
B1-M1_8	42.96	–	–	–	–	–	–
B1-M1_9	44.72	–	–	–	–	–	–
B1-M1_10	43.70	–	–	–	–	–	–
Mean values	**42.36**		**40.11**		**43.21**		**44.48**
	42.49						

Table 11. Young's moduli [GPa] for the beams made from mixture II.

Sample	$\overline{E}$	Sample	$\overline{E}$	Sample	$\overline{E}$	Sample	$\overline{E}$
B1-M2_2	46.39	B2-M2_2	43.05	B3-M2_2	46.46	B4-M2_2	44.61
B1-M2_3	45.41	B2-M2_3	46.81	B3-M2_3	50.19	B4-M2_3	47.35
B1-M2_4	52.63	B2-M2_4	51.14	B3-M2_4	45.74	B4-M2_4	52.10
B1-M2_5	54.31	B2-M2_5	52.96	B3-M2_5	47.38	B4-M2_5	52.26
B1-M2_6	56.21	–	–	–	–	–	–
Mean values	**50.99**		**48.49**		**47.44**		**49.08**
	49.12						

5.4. Two-scale analysis of the beams from the laboratory tests

This part of the paper presents the results of numerical simulations of beams of dimensions 10×15×200 cm made from two RPC mixtures, which were subjected to laboratory tests. For the purpose of the two-scale analysis, ten RVEs were generated for each mixture by means of the stochastic generator of microstructure geometry [1, 3] (Figs. 13 and 15). The amounts of particular concrete components precisely reflect the proposed RPC recipes (Table 2). It was assumed that the cement matrix consisted of: cement, silica powder, water and superplasticizer. The material parameters of the components were adopted from the publication [13]. The beams were divided at the macro scale into twenty rectangular finite elements (Fig. 12). The unit point force $P = 1$ MN was used in the calculations

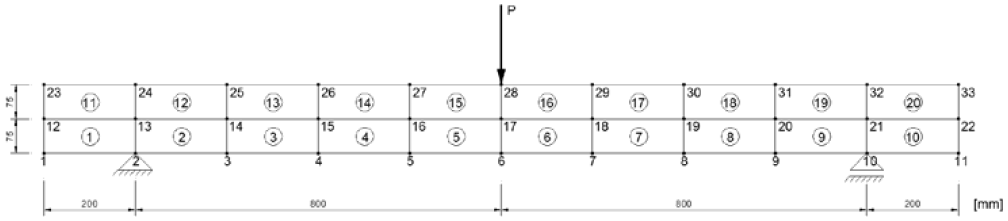

FIG. 12. The discretization of the beam on macro level.

Mixture I

The following designations have been adopted (Fig. 13):

- Red colour represents the cement matrix – percent amount 49.8%,
- Dark blue colour represents fine quartz sand – percent amount 37.4%,
- Pink colour represents steel micro fibres – percent amount 8.8%,
- Yellow colour represents air voids – percent amount 4%.

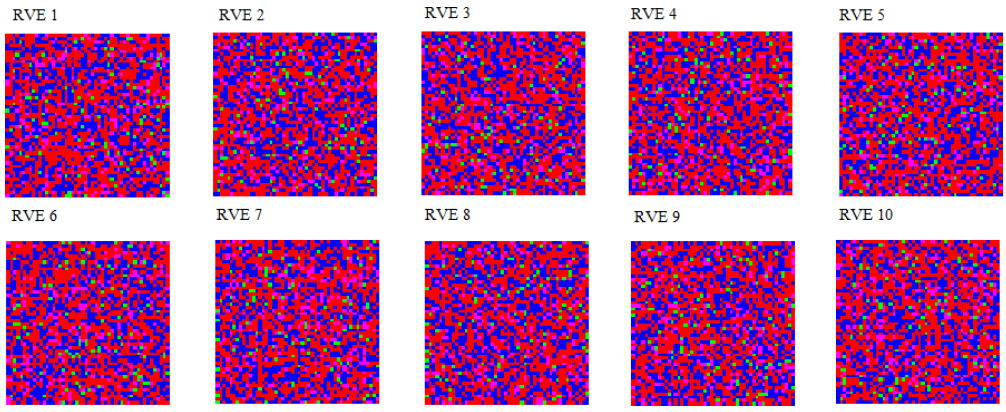

FIG. 13. Randomly generated RVEs (Mixture I).

The parameters of micro-components:

- Cement matrix $E = 29900$ MPa, $\nu = 0.24$,
- Fine quartz sand $E = 48200$ MPa, $\nu = 0.20$,
- Steel micro fibres $E = 205000$ MPa, $\nu = 0.30$,
- Air voids – empty space, no finite elements.

Figure 14 shows a visualisation of the displacements of the beam obtained with the CH_v_1.4.2 software. Its source code is included in the publication [3].

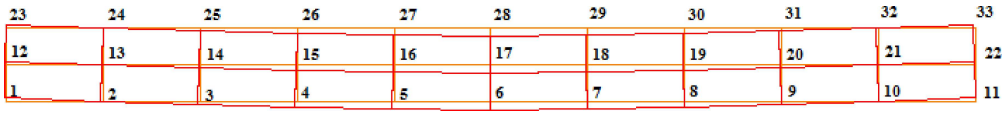

FIG. 14. A visualisation of the macro displacements of the beam (generated with the CH_v_1.4.2 program).

Mixture II

The following designations have been adopted (Fig. 15):

- Red colour represents the cement matrix – percent amount 48.2%,
- Sky blue colour represents thick quartz sand – percent amount 12.3%,
- Dark blue colour represents fine quartz sand – percent amount 22.6%,
- Pink colour represents steel micro fibres – percent amount 8.6%,
- Orange colour represents steel fibres – percent amount 4.3%,
- Yellow colour represents air voids – percent amount 4%.

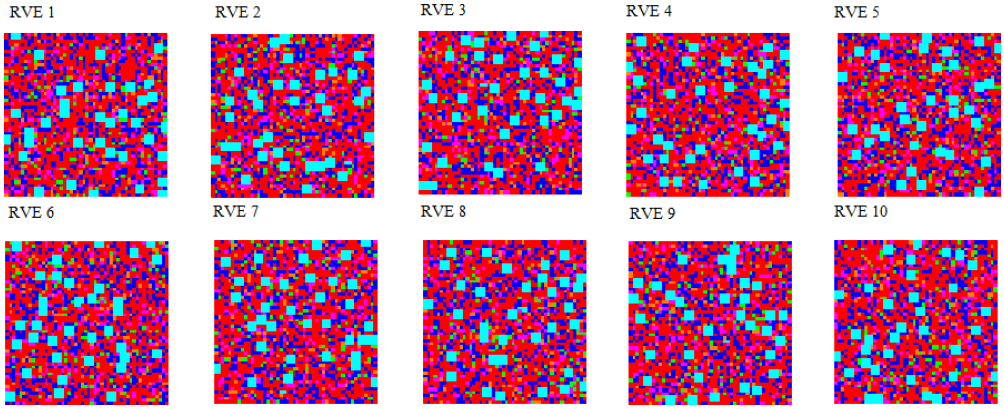

FIG. 15. Randomly generated RVEs (Mixture II).

The parameters of micro-components:

- Cement matrix $E = 29900$ MPa, $\nu = 0.24$,
- Thick quartz sand $E = 73200$ MPa, $\nu = 0.20$,
- Fine quartz sand $E = 48200$ MPa, $\nu = 0.20$,

- Steel micro fibres $E = 205000$ MPa, $\nu = 0.30$,
- Steel fibres $E = 205000$ MPa, $\nu = 0.30$,
- Air voids – empty space, No finite element.

The results of the numerical simulations conducted to determine material parameters at the macro scale are presented in Tables 12 and 13 and Figs. 16 and 17.

6. Validation of the RPC model

The validation of the RPC model presented in the papers [1, 2] is done to check whether the adopted assumptions and algorithms make it possible to correctly simulate the behaviour of structures made of reactive powder concrete within the linear elastic response. A comparison of the results of numerical simulations and those of experiments will allow us to validate the numerical model of the investigated composite material. The main goal of the research was to determine effective constitutive parameters for RPC at the macro level by means of two-scale analysis. Tables 12 and 13 contain the values of Young's modulus, Poisson's ratio and Kirchhoff's modulus determined through a two-scale analysis with the CH_v_1.4.2 software and through experiments.

Table 12. Validation of RPC – mixture I.

Sample (Fig. 15)	Young's modulus $\overline{E}$ [GPa]	Poisson's ratio $\overline{\nu}$ [–]	Kirchhoff's modulus $\overline{G}$ [GPa]
Mixture I			
RVE 1	42.20	0.22	17.26
RVE 2	40.13	0.22	16.47
RVE 3	40.23	0.22	16.54
RVE 4	41.38	0.22	16.97
RVE 5	42.84	0.23	17.48
RVE 6	44.22	0.23	17.97
RVE 7	42.67	0.22	17.52
RVE 8	42.46	0.22	17.37
RVE 9	41.62	0.22	17.07
RVE 10	39.53	0.22	16.26
Average values of the parameters obtained through a two-scale analysis	**41.73**	**0.22**	**17.09**
Average values of the parameters obtained through experiments	**42.49**	**0.20**	**17.70**
Relative error [%]	**1.79**	**10.00**	**3.45**

Table 13. Validation of the RPC model – mixture II.

Sample (Fig. 15)	Young's modulus $\overline{E}$ [GPa]	Poisson's ratio $\overline{\nu}$ [–]	Kirchhoff's modulus $\overline{G}$ [GPa]
Mixture II			
RVE 1	49.84	0.22	20.48
RVE 2	45.88	0.22	18.76
RVE 3	44.15	0.22	18.04
RVE 4	44.96	0.23	18.35
RVE 5	46.09	0.22	18.85
RVE 6	45.39	0.22	18.63
RVE 7	47.53	0.22	19.43
RVE 8	46.76	0.22	19.22
RVE 9	46.05	0.23	18.73
RVE 10	4472	0.22	18.27
Average values of the parameters obtained through a two-scale analysis	**46.14**	**0.22**	**18.88**
Average values of the parameters obtained through experiments	**49.12**	**0.32**	**18.61**
Relative error [%]	**6.07**	**31.25**	**1.45**

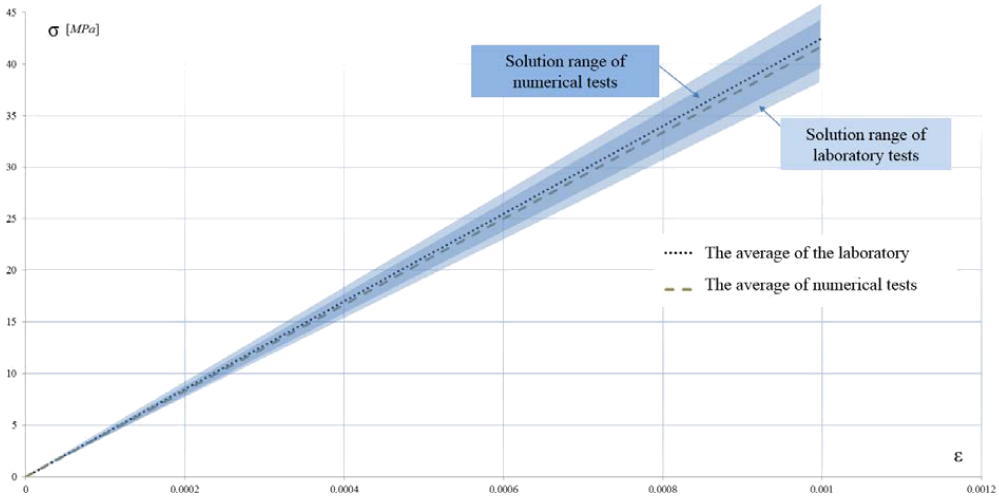

FIG. 16. Validation of results in graphical form for mixture I.

The relative error was calculated by the formula

$$\delta = \frac{\mathrm{P} - \mathrm{P}_0}{\mathrm{P}_0} \cdot 100\%, \tag{6.1}$$

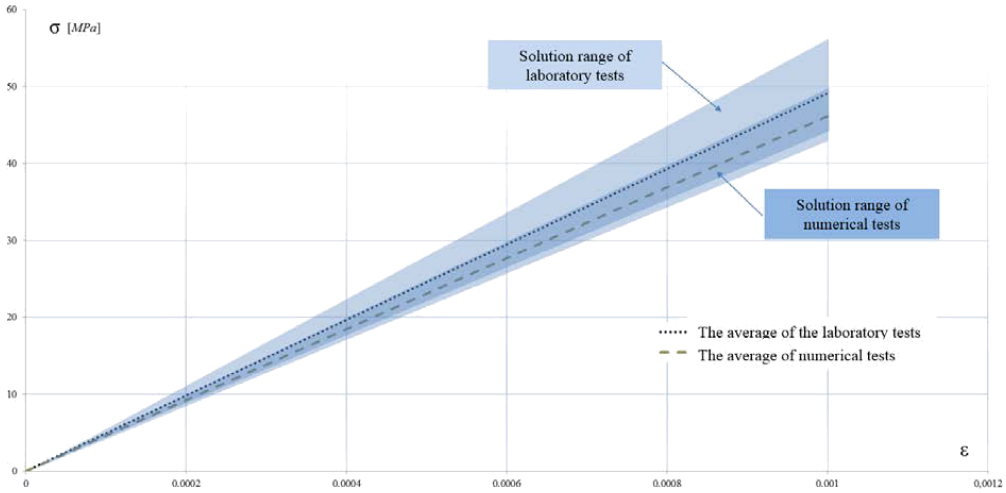

FIG. 17. Validation of results in graphical form for mixture II.

where P – the value of a parameter calculated through a two-scale analysis, P_0 – the value of a parameter calculated through laboratory experiments.

On the basis of the collected data a comparative analysis has been prepared in graphical form (Figs. 16 and 17). For the sake of clarity all straight lines corresponding to particular tests have been removed from the diagrams. The areas from which the lines were removed are marked in light blue for the results obtained through laboratory tests and in dark blue for the numerical solution, respectively The diagrams also present averaged relationships $\sigma - \varepsilon$.

7. Conclusions

On the basis of the results of the performed analysis and experiments of this three-part series about reactive powder concrete, we can formulate the following main conclusions:

- It is possible to manufacture reactive powder concrete of compressive strength of the order of 140 MPA, flexural strength – 18 MPa, and elasticity modulus – 50 GPa, without special treatments of heat or high-pressure.
- It is possible to effectively determine the macroscopic constitutive relations for reactive powder concrete on the basis of an analysis of its microstructure by using a two-scale modelling technique (numerical homogenization).
- The developed stochastic model of the microstructure of reactive powder concrete works properly for RPC beams in the elastic range, which was confirmed by the experimental tests and the validation procedure.

Acknowledgment

The conducted experimental tests were made possible thanks to the laboratory equipment purchased within the project *"Modernisation and development of the research laboratory of the Institute of Building Engineering of Zielona Góra University"* which was financed by the European Union and the Polish Government (Head of project: prof. Mieczysław Kuczma).

References

1. Denisiewicz A., Kuczma M., *Two-scale modelling of reactive powder concrete. Part I: representative volume element and solution of the corresponding boundary value problem*, Civil and Environmental Engineering Reports, **10**, 41–61, 2013.
2. Denisiewicz A., Kuczma M., *Two-scale modelling of reactive powder concrete. Part II: numerical simulations*, Engineering Transactions, **63**, 1, 35–54, 2015.
3. Denisiewicz A., *Modelowanie dwuskalowe związków konstytutywnych betonu z proszków reaktywnych i ich walidacja doświadczalna* [in Polish], PhD thesis, Supervisor prof. M. Kuczma, University of Zielona Góra, 2013.
4. Franczyk M., Prokopski G., *Optymalizacja składu betonów wysokowartościowych*, Przegląd Budowlany, **2**, 26–30, 2008.
5. http://www.gom.com/metrology-systems/system-overview/aramis.html
6. Jasiczak J., Wdowska A., Rudnicki T., *Betony ultrawysokowartościowe. Właściwości, technologie, zastosowania* [in Polish], Stowarzyszenie Producentów Cementu, Kraków, 2008.
7. Larrard F.D., *The Influence of Mix Composition on Mechanical Properties of High-Performance Silica Fume Concrete*, 4th Int. Conf. on Fly Ash, Silica Fume, Slag and Natural Pozzolans in Concrete, Istanbul, 1992.
8. PN-EN 12390-1 Badania betonu Część 1: Kształt, wymiary i inne wymagania dotyczące próbek do badania i form.
9. PN-EN 12390-2 Badania betonu Część 2: Wykonywanie i pielęgnacja próbek do badań wytrzymałościowych.
10. PN-EN 12390-3 Badania betonu Część 3: Wytrzymałość na ściskanie próbek do badania.
11. PN-EN 12390-4 Badania betonu Część 4: Wytrzymałość na ściskanie. Wymagania dla maszyn wytrzymałościowych.
12. PN-EN 12390-5 Badania betonu Część 5: Wytrzymałość na zginanie próbek do badania.
13. Sorelli L., Constantinides G., Ulm F.J., Toutlemonde F., *The nano-mechanical signature of Ultra High Performance Concrete by statistical nanoindentation techniques*, Cement and Concrete Research, **38**, 1447–1456, 2008.
14. Śliwiński J., *Ogólne zasady projektowania betonów wysokowartościowych* [in Polish], Budownictwo Technologie Architektura, Numer specjalny: Domieszki do betonu, 29–31, 2003.
15. Śliwiński J., *Zasady projektowania składu betonów wysokowartościowych* [in Polish], Cement wapno beton, **6**, 2003.